JOURNAL OF Applied Polymer SCIENCE

Electrospinning of Polymer Nanofibers Loaded with Noncovalently Functionalized Graphene

Sriya Das,[1] Ahmed S. Wajid,[1] Sanjoy K. Bhattacharia,[1] Michael D. Wilting,[2] Iris V. Rivero,[3] Micah J. Green[1]

[1]Department of Chemical Engineering, Texas Tech University, Lubbock, Texas 79409
[2]Department of Industrial Engineering, Texas Tech University, Lubbock, Texas 79409
[3]Industrial and Manufacturing Systems Engineering, Iowa State University, Ames, Iowa 50011
Correspondence to: M. J. Green (E-mail: micah.green@ttu.edu)

ABSTRACT: Pristine graphene/polyvinyl alcohol (PVA) nanofibers were prepared by electrospinning an aqueous solution of polyvinylpyrrolidone-stabilized graphene and PVA. This is the first report of electrospun nanofibers reinforced with dispersed pristine graphene. We examine the relationship between graphene loading and critical electrospinning parameters. Microscopy indicates uniform fiber formation and excellent graphene dispersion within the fiber. Rheological data indicates that the excellent level of graphene dispersion enhances the modulus of the polymer by 205%. We also find that the graphene significantly increases the fibers' thermal stability (increase of 15°C) and crystallinity (59% increase) above the baseline. In fact, the graphene may act as nucleating points for increased crystallinity. These graphene/polymer nanofibers have the potential to serve in a variety of applications, including electrodes, conductive wires, and biomedical materials. © 2012 Wiley Periodicals, Inc. J. Appl. Polym. Sci. 128: 4040–4046, 2013

KEYWORDS: electrospinning; fibers; composites; colloids

Received 5 June 2012; accepted 4 October 2012; published online 4 November 2012
DOI: 10.1002/app.38694

INTRODUCTION

Electrospinning is a versatile method of producing ultrathin fibers from a variety of precursor materials. In this process, fibers are generated by the application of electrostatic forces to a jetting polymer solution. The incorporation of nanofillers into electrospun fibers enhances the fiber properties relevant to a number of applications, particularly mechanically reinforced composites,[1] conductive membranes for fuel cell applications,[2] separation membranes,[3] protective barrier membranes, thin film batteries, tissue scaffolding, wound dressings, cardiac valve membranes, and protective clothing due to the mats' high specific surface area, controllable size, and large porosity.[4,5]

The basic principles of electrospinning are described in the Supporting Information (Figure S1). This technique is used to create nanofibers from a wide range of natural and synthetic polymers including polyacrylonitrile, polyurethane, polycarbonate, polyvinyl alcohol (PVA), poly(methyl methacrylate), and polystyrene, among others.[6–12] Similarly, biopolymers and blends of biopolymers such as poly(lactic acid) (PLA), polycaprolactone (PCL), and others have been processed into nanofibers by electrospinning for biomedical applications.[13,14]

In the present study, we examine the prospect of electrospun graphene/polymer nanocomposite fibers. Graphene is a single sheet of sp^2 bonded carbon atoms arranged into a honeycomb lattice like structure. Since its identification in the year 2004, graphene has drawn considerable interest as multifunctional nanofiller due to its combination of exceptional mechanical strength, electrical conductivity, and thermal conductivity at a relatively low cost.[15–18] Electrospinning requires that the graphene sheets first be dispersed in the polymer solution. However, there have been a number of difficulties associated with dispersing pristine graphene in a solvent; graphene sheets tend to aggregate due to attractive van der Waals forces. The most common technique used to overcome this problem is chemical modification of the graphene sheets. In this technique, graphite is initially oxidized to graphite oxide, which can be exfoliated in water to produce graphene oxide (GO). The GO may be further chemically or thermally restored to yield reduced graphene oxide (RGO). However, RGO retains some of the defects of the GO and lacks the unique properties of pristine, unfunctionalized graphene. Furthermore, recent evidence indicates the unintended production of oxidative debris during the oxidation process.[19]

Additional Supporting Information may be found in the online version of this article.

Although a range of studies have examined the use of carbon nanotubes as nanofiller in electrospun polymer fibers,[5,20–23] very few studies have actually examined the possibility of using graphene derivatives in this role.[24] Bao *et al.* reported GO/poly (vinyl acetate) (PVAc) electrospun nanocomposites where GO was chiefly used to enhance the optical properties of the composite.[25] Zhu *et al.* reported GO-embedded $Li_4Ti_5O_{12}$ (LTO) nanofibers for lithium-ion battery applications.[26] Various studies have utilized commercially available and micromechanically cleaved graphene as a nanofiller for electrospun wound dressings and photocatalysis materials.[27,28] However, prior to the present work, there have been no reports of electrospun nanofibers reinforced by stably dispersed pristine graphene.

To avoid the assorted problems associated with GO and RGO discussed above, we opted to use pristine graphene in our study.[29,30] In our previous work, we successfully demonstrated a simple and effective method to disperse pristine graphene using a polymer, polyvinylpyrrolidone (PVP).[31] This stabilizer is known to noncovalently functionalize the graphene surface and stabilize the graphene dispersion against aggregation in a range of solvents including water. In the present study, these stabilized pristine graphene dispersions were utilized for producing graphene/polymer electrospun mats. PVA was selected as the matrix for the PVP-stabilized graphene electrospun fibers because of its biocompatibility and range of applications. (Note that prior studies have demonstrated excellent compatibility between PVA and PVP.[32]) Below we also identify the critical electrospinning parameters that affect morphology and properties of the resultant pristine graphene-loaded fibers.

EXPERIMENTAL

Expanded graphite (EG) (grade-3805) was provided by Asbury Carbons. Polyvinylpyrrolidone (PVP) (M_W: 10,000 g mol^{-1}) and polyvinyl alcohol (PVA) (M_w ~89,000–98,000 g mol^{-1}) 99+ % hydrolyzed, was purchased from Sigma–Aldrich.

Sample Preparation

Stable graphene dispersions were prepared by adding 40 mg mL^{-1} of expanded graphite (EG) to the PVP solution in water (10 mg mL^{-1}). The solution was tip sonicated using a Misonix sonicator (XL 2000) at output wattage of 10 W for 1 h at room temperature. The dispersions were then centrifuged at ~5000 rpm for 4 h to remove aggregates. It has been demonstrated in the past that this method yields noncovalently functionalized graphene dispersions.[31,33]

The supernatant liquid obtained was mixed with aqueous PVA solutions (8 wt %) and stirred for 1 h to obtain the viscous solution for electrospinning. The prepared solution had a graphene loading of 0.5 wt % (dry basis). An 8 wt % PVA solution in water was used as the baseline sample for comparison. In both the baseline and the graphene loaded sample, the amount of PVP was maintained equally.

Electrospinning

The solution was loaded into hypodermic syringes fitted with blunt needles (Gauge$18^{1/2}$). A syringe pump (Chemyx, Inc Fusion 200) was used to control the flow rate of the solution. The applied voltage was adjusted between 10 and 20 kV. Fibers were collected on a grounded metal collector (wrapped with an aluminum foil) which was varied between 12 and 15 cm away from the needle on distinct runs.

Characterization

The morphology of the graphene/PVA fibers were investigated by optical microscopy and scanning electron microscopy (SEM, Hitachi S4300 SE/N). SEM samples were prepared by sputter coating with Au/Pd in Hummer V Technics sputter coater at 10 kV and 10 mA current for 1.5 min at a rate of 10 nm min^{-1}. High resolution transmission electron microscopy (HRTEM) (Hitachi, H8100) was performed to analyze the dispersion of graphene in the polymer fibers. The fibers were placed on carbon-coated copper grids for HRTEM. Thermogravimetric Analysis (TGA) was performed in a Instrument Specialist instrument to determine the thermal stability of the fiber mats. TGA samples (~15 mg) were heated from room temperature to 800°C at a rate of 10°C min^{-1} in a nitrogen atmosphere. The degradation temperatures were obtained from the differential TGA curve. X-ray diffraction (XRD) was performed in a PANalytical X'Pert Pro MPD (with an accelerator detector) using Ni-filtered Cu Kα radiation (α = 1.54 Å) operated at 45 kV and 40 mA current. Melt rheological experiments were performed using a parallel plate fixture (CTD450 + PP-25) on a shear rheometer (Anton Paar, USA). The changes in glass transition temperature and crystallization behavior due to graphene loading were examined by DSC (TA instrument, Model Q-20-1848) instrument. The samples (~5 mg) were sealed in aluminum pans (40 μL) and experiments were conducted in nitrogen atmosphere at heating and cooling rates of 10°C min^{-1}. To eliminate thermal history, the samples were heated from room temperature to 90°C, maintained at this temperature for several minutes, then cooled to room temperature and heated again to 300°C. The glass transition temperature and melting enthalpy were taken from the second heating run in the calorimetric curves.

RESULTS AND DISCUSSION

In this article, we utilize polymer-stabilized graphene as nanofiller for electrospun pristine graphene/PVA fibers. These fibers could be utilized in various applications like wound dressings, water filtration, tissue engineering, and fuel cell applications.[34–36] Stable pristine graphene dispersion in water was mixed with an aqueous PVA solution to create the viscous precursor solution. The baseline PVA fibers were spun at a voltage of 10 kV, a flowrate of 0.3–0.5 mL h^{-1}, and a tip-target distance of ~10 cm. Figure 1 shows the optical microscope and transmission electron microscope (TEM) images of the baseline PVA-only fibers. The electrospun fibers have diameters at the submicron level (~0.5–0.7 μm) and did not show any bead formation. Compared to prior work on electrospun PVA,[9] our average fiber diameter was larger; this is caused by the increase in viscosity of precursor PVA solution upon addition of PVP. The increase in viscosity decreases elongation and produces larger diameter fibers.[37,38]

As expected, the addition of graphene to the PVA solution significantly altered the viscosity and solution conductivity of the polymer solution; 0.5 wt % graphene (dry basis) was used. The textural morphology of the graphene-loaded fibers was

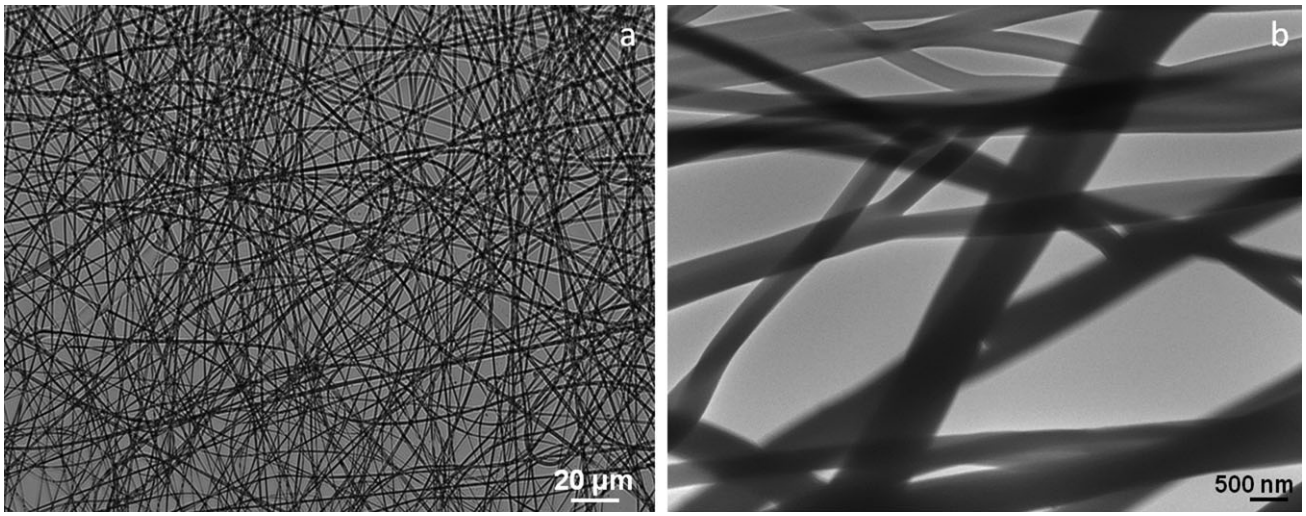

Figure 1. (a) Optical microscope and (b) high resolution TEM images of electrospun PVA mat. There was no beading observed and the fiber diameters ranged from 0.5 to 0.7 μm.

distinctly different from that of the polymer fibers. To obtain consistent, bead-free fibers, the electrospinning parameters had to be optimized. A series of experiments were performed to study the effects of flowrate, applied voltage and tip-target distance on the fiber formation. These experiments aided in achieving optimal conditions for spinning bead-free graphene/PVA/PVP fibers. The morphology of the final fibers was characterized by both optical and scanning electron microscopy as discussed below.

Relatively few studies have analyzed the effect of flowrate on fiber morphology.[39] In our work, the flowrate was changed from 0.3 to 15 mL h^{-1} to obtain bead-free graphene-loaded fibers. Supporting Information Figure S3 shows the optical microscopy images of the graphene/PVA/PVP fibers with the increase in flowrate. It was observed that at a flowrate of 15 mL h^{-1}, the fibers were free of defects. This flowrate used for spinning our fibers was relatively high, we obtained bead-free submicron-diameter pristine graphene-loaded fibers.

Also, prior reports of nanofilled electrospun fibers report similarly high values.[27] Jeong *et al.* observed beading with the incorporation of multiwalled carbon nanotubes (MWNTs), at the same spinning conditions as the baseline PVA mat.[40] The flowrate was altered from ~0.1 to 5 mL h^{-1} to obtain bead-free MWNT-loaded fibers. The addition of nanotubes to the PVA matrix considerably increased the effective fluid charge density. It was therefore necessary to change the flowrate accordingly to successfully spin the mat. Similar effects were caused by addition of graphene to the PVA matrix in our case. Hence, the optimal flowrate was increased to 15 mL h^{-1} to obtain defect-free fibers.

We observed a reduction in bead formation with the increase in applied voltage from 10 to 15 kV (Supporting Information Figure S4). This increase in voltage is required because graphene's conductivity increases the surface charge of the fiber, naturally leading to bead formation.[41] The addition of graphene also increases the elasticity of the jet; this justifies the need for a larger voltage compared to the baseline experiment. Increasing the voltage amplifies the repulsive electrostatic force and favors the formation of fibers with smaller diameters.[9] We also observed that the tip-target distance had minimal effect on the fiber diameter.

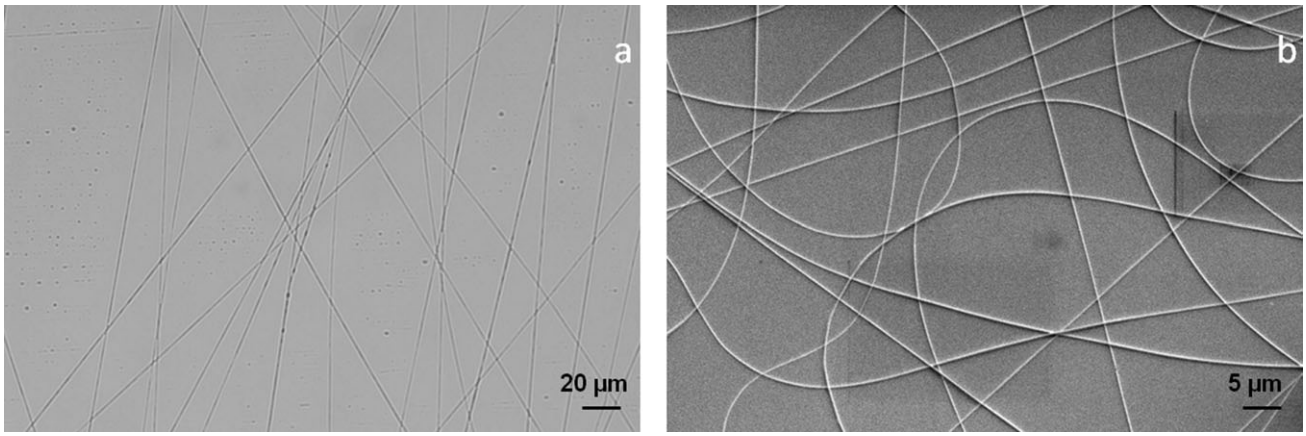

Figure 2. (a) Optical microscope and (b) SEM images of electrospun 0.5 wt % graphene/PVA mat. The fibers were bead-free and the observed fiber diameters ranged from 0.7 to 1 μm.

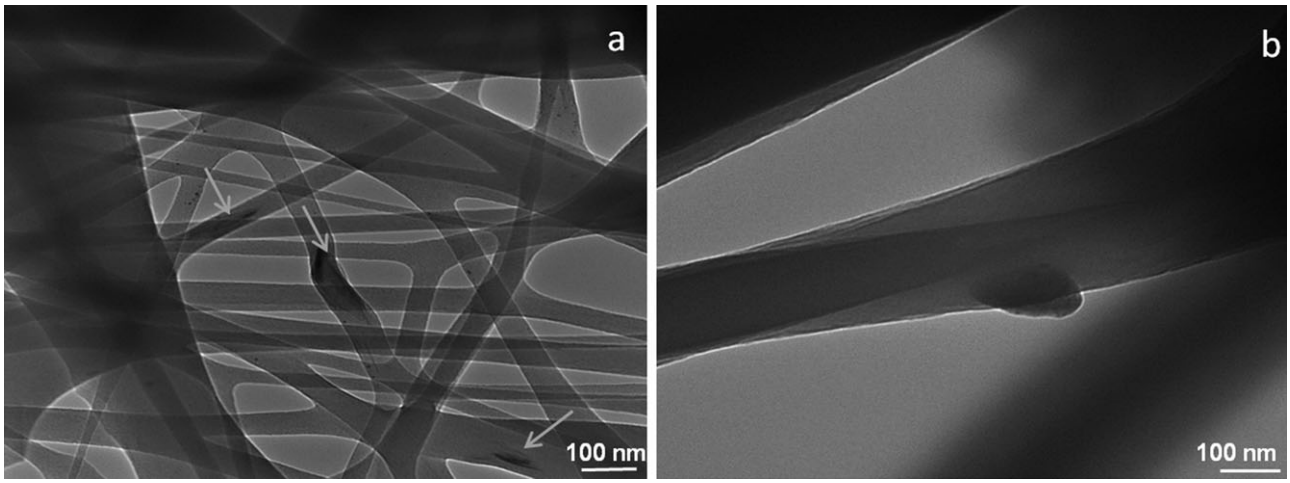

Figure 3. HRTEM images of electrospun (a) graphene/PVA/PVP mat and a (b) single graphene/PVA/PVP fiber. The graphene sheets were well distributed in the PVA matrix without aggregation (shown with green arrows). Because the lateral dimension of graphene is comparable to the fiber diameter, the graphene occasionally protrudes out of the PVA fiber as seen here.

Figure 2 shows the optical microscopy and scanning electron microscopy studies on the fibers produced using optimal voltage and flowrate values. The optical microscopy images show that spinning the fibers with the optimized parameters indeed yields defect-free fibers. For clarity, high resolution SEM imaging was performed on the fibers. Figure 2(b) shows that the final 0.5 wt % graphene/PVA/PVP fibers were bead-free and the diameter ranged from 0.7 to 1 μm.

In our previous work, we demonstrated that our technique for isolating PVP-stabilized graphene yields graphene sheets that are single to few layers thick.[31] Additional TEM images of the PVP-stabilized graphene sheets in water are provided in the Supporting Information (Figure S5). The edges of the graphene sheets as observed in the TEM images indicate that PVP does indeed stabilize single-few layer graphene in water without aggregation. HRTEM was performed on the graphene/PVA fibers to assess the dispersion quality of the graphene sheets within the PVA matrix (Figure 3). Figure 3(a) shows images of graphene/PVA fibers with a diameter of 0.4–0.7 μm. The image demonstrates that the graphene is well dispersed in the PVA matrix without aggregation. Because the lateral size of graphene is comparable to the fiber diameter, the graphene does protrude from the fiber surface in some cases. Similar effects have been observed for carbon nanotubes.[42] Additional low resolution TEM images of graphene/PVA fibers are shown in Supporting Information (Figure S6). XRD analysis also confirms excellent dispersion within the PVA matrix (Supporting Information Figure S7).

Table I. Degradation Temperature (from TGA) and Thermal Properties (from DSC) of the Baseline PVA and Graphene-Loaded PVA Fibers

Samples	T_g, °C	T_m, °C	H_m, J/g	X_c, %
PVA/PVP, baseline	74	223.73	33.12	23.0
0.5 wt % graphene/PVA	73	226.02	50.95	36.7

The thermal stability of the electrospun fibers was tested using TGA. Derivative thermogravimetry results of baseline fibers and the graphene/PVA fibers yields the peak degradation temperature of the samples (Table I, Supporting Information Figure S8). The degradation temperature for the PVA/PVP was measured to be 370°C. Thermal stability substantially improves upon addition of graphene, with a 15°C increase in the degradation temperature corresponding to a 0.5 wt % graphene loading. This enhancement of thermal stability with a low graphene loading compares well against the nanocomposites literature.[29,43–45] This indicates that graphene is well dispersed in the PVA matrix and prevents the early degradation of PVA in the baseline fibers. The degradation temperature of the baseline is higher than a typical PVA matrix. This increase is mainly due to the presence of PVP, which has a degradation temperature of 350–500°C.[46–48]

The DSC curves for baseline PVA and for electrospun graphene loaded (0.5 wt %) mats are shown in Figure 4. The glass transition temperature of these samples was obtained from the onset of the transition point and melting temperature and melting

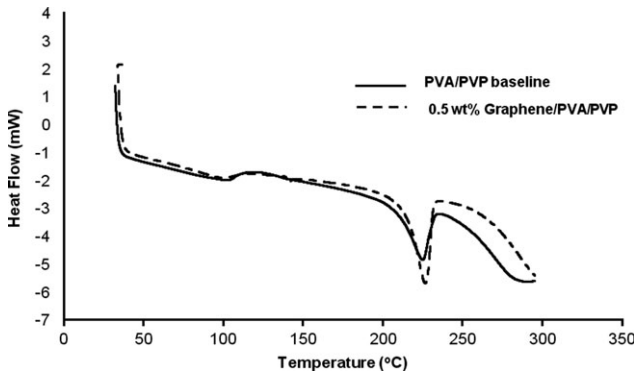

Figure 4. DSC curves of baseline PVA and graphene/PVA composites (0.5 wt % graphene content).

enthalpy were calculated from the melting peaks of the DSC curve. The results of glass transition temperature (T_g), melting temperature (T_m), melting enthalpy (ΔH_m), and degree of crystallinity (X_c) of the composites are represented in Table I. As shown in this table, no significant change in glass transition and melting temperature was observed for graphene loading in PVA. Prior studies suggest that there is interchain hydrogen bonding between the carbonyl groups of PVP and the hydroxyl groups of the PVA chains.[49] These hydrogen bonding interactions affect the mobility of the polymer chain, and only a slight increase in T_g was observed. However, it does not adversely affect the mechanical properties of the composite. Prior papers have shown similar trends in the change in glass transition temperature.[50,51]

The degree of crystallinity were calculated from the ratio between melting enthalpy of the samples (ΔH_m) and melting enthalpy of 100% crystalline PVA (ΔH_0) which is considered to be 138.6 J g^{-1}.[52,53] The crystallinity of the 0.5 wt % graphene/PVA composite increased by 59% compared to the baseline PVA/PVP mat; this indicates that the graphene is well dispersed in the PVA matrix and does not disrupt the crystallinity of PVA matrix. The prior literature includes both reports of decreases and reports of increases in the crystallinity of the matrix with increases in nanofiller loading. Jeong *et al.* have introduced pristine and functionalized multi-walled nanotubes (MWNTs) in a nylon 6,10 matrix.[40] The increase in crystallinity was higher in-case of the functionalized nanotubes which is attributed to the higher dispersibility of these tubes in the polymer matrix. The functionalized nanotubes act as nucleating points. The pristine MWNTs loaded nylon composite exhibits almost similar crystallinity as the nylon 6,10 by itself. This was due to the poor contacts between the pristine tubes and nylon. On the other hand, Jose *et al.* have argued that the incorporation of MWNTs into polypropylene fibers hinders the recrystallization of the matrix.[45] The difference between these two reports may be attributed to differences in filler–matrix interactions. In our case, the data do indicate that the interaction of the filler (graphene) with the matrix increases the crystallinity of the matrix, and graphene sheets indeed act as nucleation points in PVA composites[54] unlike other nanofillers.[55,56] However, the crystallinity values for the electrospun mats (both the baseline and the graphene loaded mat) are lower than that reported in prior electrospinning studies. This decrease in crystallinity can be attributed to the rapid solvent evaporation, miscibility of the polymers (PVA and PVP) and high flowrate used during the spinning process.[57–59]

Melt rheology was utilized to characterize the enhancement of the mechanical properties of graphene-loaded PVA. The samples were melted in the rheometer and a dynamic oscillatory shear test was conducted on the melt. We observed a considerable increase (205%) in storage modulus (G') with the incorporation of 1 wt % graphene (Supporting Information Figure S9) similar to graphene/polycarbonate composites.[60] The notable increase in storage modulus is an indication of the excellent dispersion of graphene in the matrix; the adsorbed polymer prevents any van der Waals-induced graphene aggregation. Proper dispersion of graphene in the polymer matrix is necessary for an efficient transfer of properties from graphene to the PVA matrix. This implies that the PVP-stabilized graphene exhibits excellent interfacial adhesion with the PVA matrix and enhances the mechanical properties. We expect to see similar behavior in the electrospun fibers given that the graphene is stabilized with the same polymer and spun into the same PVA matrix.

Prior studies indicate that the percolation threshold should be 0.1–0.3 vol % if the graphene is well dispersed in bulk PVA.[61,62] Such electrical measurements are notoriously difficult to make on electrospun fibers, and percolation becomes complex when the matrix and nanofiller lengthscales are comparable as seen in the TEM images.

CONCLUSIONS

In summary, we have demonstrated a simple technique to process graphene-loaded polymer nanofibers. To our knowledge, this research represents the first attempt to electrospin polymer nanofibers loaded with pristine graphene. Even at low graphene loading, the fibers exhibit a notable enhancement in thermal stability and crystallinity. The SEM, TEM, and XRD results confirm excellent dispersion quality of graphene in the polymeric solution, while optical microscopy images display uniform electrospun fiber formation without significant beading. The ultrafine graphene fibers produced by our method are highly promising for use in electrodes, conductive wires, smart fabrics, and similar applications which require conductive filler inside the polymer nanofibers. Given the biocompatible nature of PVP and PVA, the graphene/PVP/PVA electrospun fibers also show tremendous potential in biomedical applications such as tissue engineering and wound healing.

ACKNOWLEDGMENTS

The authors acknowledge Joseph Pickel and Andrew Payzant of the Center for Nanophase Materials Sciences (CNMS) at Oak Ridge National Lab for their help in TGA and XRD measurements. They acknowledge Colin Young and Professor Matteo Pasquali of Rice University for their help with the Raman measurements. They thank Joseph L. Lowery for all the helpful discussions. They also thank Fahmida Irin, Abel B. Cortinas, Robert J. Fullerton, H.S. Tanvir Ahmed, John L. Shelburne, and Fred Schneider of TTU for their help during this work. The SEM was performed at the TTU Imaging Center (funded by NSF MRI 04-511) supported by Dr. Mark J. Grimson and Professor Lauren S. Gollahon. Funding was provided by the U.S. National Science Foundation (NSF) under award CBET-1032330 and by the Air Force Office of Scientific Research Young Investigator Program (AFOSR FA9550-11-1-0027). A portion of this research was conducted at the Center for Nanophase Materials Sciences, which is sponsored at Oak Ridge National Laboratory by the Office of Basic Energy Sciences, US Department of Energy (CNMS User Nanoscience Research Program 2011-230). Additional TGA data, electrospinning schematic, HRTEM images, XRD and melt rheology data are provided in the Supporting Information.

REFERENCES

1. Chang, T. E.; Kisliuk, A.; Rhodes, S. M.; Brittain, W. J.; Sokolov, A. P. *Polymer* **2006**, *47*, 7740.

2. Kim, D. S.; Park, H. B.; Rhim, J. W.; Lee, Y. M. *J. Membr. Sci.* **2004**, *240*, 37.
3. Peng, F. B.; Hu, C. L.; Jiang, Z. Y. *J. Membr. Sci.* **2007**, *297*, 236.
4. Huang, Z.-M.; Zhang, Y. Z.; Kotaki, M.; Ramakrishna, S. *Compos. Sci. Technol.* **2003**, *63*, 2223.
5. Chronakis, I. S. *J. Mater. Process. Technol.* **2005**, *167*, 283.
6. Carol, P.; Ramakrishnan, P.; John, B.; Cheruvally, G. *J. Power Sources* **2011**, *196*, 10156.
7. Demir, M. M.; Yilgor, I.; Yilgor, E.; Erman, B. *Polymer* **2002**, *43*, 3303.
8. Shawon, J.; Sung, C. M. *J. Mater. Sci.* **2004**, *39*, 4605.
9. Zhang, C. X.; Yuan, X. Y.; Wu, L. L.; Han, Y.; Sheng, J. *Eur. Polym. J.* **2005**, *41*, 423.
10. Gupta, P.; Elkins, C.; Long, T. E.; Wilkes, G. L. *Polymer* **2005**, *46*, 4799.
11. Lee, K. H.; Kim, H. Y.; Bang, H. J.; Jung, Y. H.; Lee, S. G. *Polymer* **2003**, *44*, 4029.
12. Yang, Q. B.; Li, Z. Y.; Hong, Y. L.; Zhao, Y. Y.; Qiu, S. L.; Wang, C.; Wei, Y. *J. Polym. Sci. B Polym. Phys.* **2004**, *42*, 3721.
13. Zhou, H. J.; Kim, K. W.; Giannelis, E.; Joo, Y. L. *Polym. Nanofibers* **2006**, *918*, 217.
14. Reneker, D. H.; Kataphinan, W.; Theron, A.; Zussman, E.; Yarin, A. L. *Polymer* **2002**, *43*, 6785.
15. Novoselov, K. S.; Geim, A. K.; Morozov, S. V.; Jiang, D.; Zhang, Y.; Dubonos, S. V.; Grigorieva, I. V.; Firsov, A. A. *Science* **2004**, *306*, 666.
16. Lee, C.; Wei, X. D.; Kysar, J. W.; Hone, J. *Science* **2008**, *321*, 385.
17. Du, X.; Skachko, I.; Barker, A.; Andrei, E. Y. *Nat. Nanotechnol.* **2008**, *3*, 491.
18. Seol, J. H.; Jo, I.; Moore, A. L.; Lindsay, L.; Aitken, Z. H.; Pettes, M. T.; Li, X. S.; Yao, Z.; Huang, R.; Broido, D.; Mingo, N.; Ruoff, R. S.; Shi, L. *Science* **2010**, *328*, 213.
19. Rourke, J. P.; Pandey, P. A.; Moore, J. J.; Bates, M.; Kinloch, I. A.; Young, R. J.; Wilson, N. R. *Angew. Chem. Int. Edit.* **2011**, *50*, 3173.
20. Bounioux, C.; Itzhak, R.; Avrahami, R.; Zussman, E.; Frey, J.; Katz, E. A.; Yerushalmi-Rozen, R. *J. Polym. Sci. B Polym. Phys.* **2011**, *49*, 1263.
21. Prilutsky, S.; Zussman, E.; Cohen, Y. *J. Polym. Sci. B Polym. Phys.* **2010**, *48*, 2121.
22. Rein, D. M.; Cohen, Y.; Lipp, J.; Zussman, E. *Macromol. Mater. Eng.* **2010**, *295*, 1003.
23. Hou, H. Q.; Ge, J. J.; Zeng, J.; Li, Q.; Reneker, D. H.; Greiner, A.; Cheng, S. Z. D. *Chem. Mater.* **2005**, *17*, 967.
24. Mack, J. J.; Viculis, L. M.; Ali, A.; Luoh, R.; Yang, G. L.; Hahn, H. T.; Ko, F. K.; Kaner, R. B. *Adv. Mater.* **2005**, *17*, 77.
25. Bao, Q. L.; Zhang, H.; Yang, J. X.; Wang, S.; Tong, D. Y.; Jose, R.; Ramakrishna, S.; Lim, C. T.; Loh, K. P. *Adv. Funct. Mater.* **2010**, *20*, 782.
26. Zhang, X. T.; Sui, Z. Y.; Xu, B.; Yue, S. F.; Luo, Y. J.; Zhan, W. C.; Liu, B. *J. Mater. Chem.* **2011**, *21*, 6494.
27. Kim, C. H.; Kim, B.-H.; Yang, K. S. *Carbon.* **2012**, *50*, 2472–2481.
28. Lu, B.; Li, T.; Zhao, H.; Li, X.; Gao, C.; Zhang, S.; Xie, E. *Nanoscale* **2012**, *4* 2978–2982.
29. Das, S.; Irin, F.; Tanvir Ahmed, H. S.; Cortinas, A. B.; Wajid, A. S.; Parviz, D.; Jankowski, A. F.; Kato, M.; Green, M. J. *Polymer* **2012**, *53*, 2485.
30. Das, S.; Wajid, A. S.; Shelburne, J. L.; Liao, Y.-C.; Green, M. J. *ACS Appl. Mater. Interfaces* **2011**, *3*, 1844.
31. Wajid, A. S.; Das, S.; Irin, F.; Ahmed, H. S. T.; Shelburne, J. L.; Parviz, D.; Fullerton, R. J.; Jankowski, A. F.; Hedden, R. C.; Green, M. J. *Carbon* **2012**, *50*, 526.
32. Jones, S. A.; Martin, G. P.; Royall, P. G.; Brown, M. B. *J. Appl. Polym. Sci.* **2005**, *98*, 2290.
33. Bourlinos, A. B.; Georgakilas, V.; Zboril, R.; Steriotis, T. A.; Stubos, A. K.; Trapalis, C. *Solid State Commun.* **2009**, *149*, 2172.
34. Li, D.; Xia, Y. *Adv Mater* **2004**, *16*, 1151.
35. Bao, Q.; Zhang, H.; Yang, J.-X.; Wang, S.; Tong, D. Y.; Jose, R.; Ramakrishna, S.; Lim, C. T.; Loh, K. P. *Adv. Funct. Mater.* **2010,** *20,* 782–791.
36. Zhu, N.; Liu, W.; Xue, M.; Xie, Z.; Zhao, D.; Zhang, M.; Chen, J.; Cao, T. *Electrochim. Acta* **2012,** *55,* 5813–5818.
37. McKee, M. G.; Wilkes, G. L.; Colby, R. H.; Long, T. E. *Macromolecules* **2004**, *37*, 1760.
38. Ki, C. S.; Baek, D. H.; Gang, K. D.; Lee, K. H.; Um, I. C.; Park, Y. H. *Polymer* **2005**, *46*, 5094.
39. Pham, Q. P.; Sharma, U.; Mikos, A. G. *Tissue Eng.* **2006**, *12*, 1197.
40. Jeong, J. S.; Moon, J. S.; Jeon, S. Y.; Park, J. H.; Alegaonkar, P. S.; Yoo, J. B. *Thin Solid Films* **2007**, *515*, 5136.
41. Rutledge, G. C.; Fridrikh, S. V. *Adv. Drug Deliv. Rev.* **2007**, *59*, 1384.
42. Ko, F.; Gogotsi, Y.; Ali, A.; Naguib, N.; Ye, H. H.; Yang, G. L.; Li, C.; Willis, P. *Adv. Mater.* **2003**, *15*, 1161.
43. Gao, J. B.; Itkis, M. E.; Yu, A. P.; Bekyarova, E.; Zhao, B.; Haddon, R. C. *J. Am. Chem. Soc.* **2005,** *127,* 3847–3854.
44. Kim, H.-S.; Park, B. H.; Yoon, J.-S.; Jin, H.-J. *Mater. Lett.* **2007,** *61,* 2251–2254.
45. Jose, M. V.; Dean, D.; Tyner, J.; Price, G.; Nyairo, E. *J. Appl. Polym. Sci.* **2007**, *103*, 3844.
46. Du, Y. K.; Yang, P.; Mou, Z. G.; Hua, N. P.; Jiang, L. *J. Appl. Polym. Sci.* **2006**, *99*, 23.
47. Bogatyrev, V. M.; Borisenko, N. V.; Pokrovskii, V. A., *Russ. J. Appl. Chem.* **2001**, *74*, 839.
48. Zheng, M. P.; Gu, M. Y.; Jin, Y. P.; Jin, G. L. *Mater. Sci. Eng. B Solid State Mater. Adv. Technol.* **2000**, *77*, 55.
49. Huang, Y.; Zheng, Y.; Song, W.; Ma, Y.; Wu, J.; Fan, L. *Compos. A Appl. Sci. Manufact.* **2011**, *42*, 1398.
50. Jiang, L.; Shen, X.-P.; Wu, J.-L.; Shen, K.-C. *J. Appl. Polym. Sci.* **2010**, *118*, 275.
51. Liang, J.; Huang, Y.; Zhang, L.; Wang, Y.; Ma, Y.; Guo, T.; Chen, Y. *Adv. Funct. Mater.* **2009**, *19*, 2297.

52. Cerezo, F. T.; Preston, C. M. L.; Shanks, R. A. *Macromol. Mater. Eng.* **2007**, *292*, 155.

53. Su, J.; Wang, Q.; Su, R.; Wang, K.; Zhang, Q.; Fu, Q. *J. Appl. Polym. Sci.* **2008**, *107*, 4070.

54. Zhao, X.; Zhang, Q.; Chen, D.; Lu, P. *Macromolecules* **2010**, *43*, 2357.

55. Chatterjee, S.; Nueesch, F. A.; Chu, B. T. T. *Nanotechnology* **2011,** *22,* 222011. DOI: 10.1088/0957-4484/22/27/275714.

56. Liang, G.; Xu, J.; Xu, W.; Shen, X.; Zhang, H.; Yao, M. *Polym. Compos.* **2011,** *32,* 511–518.

57. Huang, Z. M.; Zhang, Y. Z.; Kotaki, M.; Ramakrishna, S. *Compos. Sci. Technol.* **2003**, *63*, 2223.

58. Thomas, V.; Jose, M. V.; Chowdhury, S.; Sullivan, J. F.; Dean, D. R.; Vohra, Y. K. J. *Biomater. Sci. Polym. Ed.* **2006**, *17*, 969.

59. Subbiah, T.; Bhat, G. S.; Tock, R. W.; Pararneswaran, S.; Ramkumar, S. S. *J. Appl. Polym. Sci.* **2005**, *96*, 557.

60. Kim, H.; Macosko, C. W. *Polymer* **2009,** *50,* 3797–3809.

61. McCullen, S. D.; Stevens, D. R.; Roberts, W. A.; Ojha, S. S.; Clarke, L. I.; Gorga, R. E. *Macromolecules* **2007,** *40,* 997–1003.

62. Stankovich, S.; Dikin, D. A.; Piner, R. D.; Kohlhaas, K. A.; Kleinhammes, A.; Jia, Y.; Wu, Y.; Nguyen, S. T.; Ruoff, R. S. *Carbon* **2007**, *45*, 1558.